

Atomistic Molecular Dynamics Simulations of the Interactions of Oleic and 2-Hydroxyoleic Acids with Phosphatidylcholine Bilayers

Javier Cerezo,* José Zúñiga,* Adolfo Bastida, and Alberto Requena*

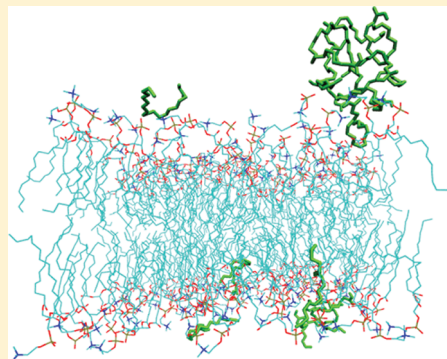
Departamento de Química Física, Universidad de Murcia, 30100 Murcia, Spain

José Pedro Cerón-Carrasco

CEISAM, UMR CNRS 6230, BP 92208, Université de Nantes, 2, rue de la Houssinière, 44322 Nantes Cedex 3, France

 Supporting Information

ABSTRACT: Fatty oleic acid (OA) and, recently, its derivative 2-hydroxyoleic acid (2OHOA) have been reported to display an important therapeutic activity. To understand better these therapeutic effects at the molecular and cellular levels, in this work we have carried out molecular dynamics simulations to elucidate the structural and dynamical changes taking place in model 1,2-dimyristoyl-*sn*-glycero-3-phosphocholine (DMPC) and 1,2-dipalmitoyl-*sn*-glycero-3-phosphocholine (DPPC) bilayers upon insertion of rising concentrations of these two fatty acids. The simulations are performed using a united-atoms model to describe both the phospholipids and the fatty acids. The process of insertion of the fatty acids from the aqueous phase into the bilayers is simulated first, showing that it is feasible and may lead to some degree of phase separation within the bilayer. The interactions of the embedded homogeneously dispersed fatty acids with the phospholipid chains of the bilayers are then simulated at different concentrations of the fatty acids. The results from these simulations show that accumulation of OA and 2OHOA up to high concentrations induces only small structural changes in the bilayers. An increase of the mobility of the lipid and fatty acid chains at rising fatty acid concentrations is also observed, which is more marked for the fatty acid chains, along with an enhancement of the permeability of the bilayers to the hydrophobic penetrant.



I. INTRODUCTION

Cell membranes are complex biological structures consisting of a phospholipid bilayer in which a variety of other biomolecules are immersed. Among the most relevant components of bio-membranes are cholesterol, which regulates the fluidity of the membrane,¹ proteins, which are involved in a number of physiological functions,² and fatty acids, which are able to modulate the lipid organization inside the membrane.³

The large amount of cellular processes in which membranes participate has prompted the emergence of a new therapeutic field known as membrane lipid therapy,³ based on inducing alterations within the membranes that have a desirable effect on the processes that they regulate. These therapies make accordingly wide use of new drugs able to interact with the membranes and modify their structural and dynamical properties. Fatty acids (FAs) stand then as very promising candidates to be used for the purpose since they have been reported to affect the properties of biological membranes appreciably,³ with their impact being more significant when the fatty acid chains have a “kinked” *cis*-double bond structure, as in the case of the 9-*cis*-octadecanoic acid, or oleic acid (OA).^{4,5} This fatty acid is, in fact, one of the most abundant in nature and has been widely demonstrated to have beneficial properties for human health.^{6,7} One of the most important sources of oleic acid is olive oil, which is widely present in the Mediterranean diet. Not surprisingly

then, this diet has been shown to lead to high concentrations of OA in plasma membranes,⁸ which have been subsequently correlated with an important reduction of the risk of developing cardiovascular diseases and cancer.^{9–13} Quite recently also, a synthetic derivative of OA, the 2-hydroxyoleic acid (2OHOA), has been reported as having a strong antihypertensive action^{14,15} and to prevent cancer.^{14,16,17} These therapeutic properties of 2OHOA have accompanied the observation that this fatty acid induces the formation of H_{II} structures in model membranes¹⁸ and that it alters the lipid composition of certain plasma membranes.^{19,20}

The health benefits associated with oleic acid and its derivatives have spawned a number of studies, both experimental and theoretical, investigating the changes produced by these fatty acids in lipid membranes.^{21–28,18,20,29–38} Experimentally, it has been observed using X-ray diffraction and differential scanning calorimetry (DSC) that these unsaturated fatty acids reduce the temperature at which the phase transition from the lamellar-gel (L_β) and lamellar-fluid (L_α) phases to the nonlamellar hexagonal (H_{II}) phases takes place in a variety of membranes^{25–28,18,34,36,38} and also that they induce some structural modifications in the membranes.^{27,18,36}

Received: April 14, 2011

Revised: August 31, 2011

Published: September 01, 2011

Moreover, the extra stabilization of the nonlamellar phases has been shown to be correlated with changes in the action of some membrane proteins.¹⁹

From the theoretical point of view, Knecht et al.³¹ have simulated using molecular dynamics (MD) the phase transitions occurring in model systems formed by a DPPC bilayer and palmitic acid in water, at different temperatures and initial configurations. These simulations show in atomic detail how the phase transition from the gel phase (L_β) to the nonlamellar inverted hexagonal phase takes place at around 330 K, in good agreement with experiment. In systems with a major presence of saturated fatty acids, such as palmitic, the most stable phases are indeed the gel and the nonlamellar hexagonal phases. At physiological temperatures, however, cell membranes are commonly in the fluid phase (L_α).³⁹ For this reason, the theoretical studies that explore the effect of unsaturated fatty acids on the structure of cell membranes are carried out on model bilayers maintained in the fluid phase by an adequate setting of the temperature.^{32,36–38} Following this approach, Notman et al.³² have studied the interactions of oleic acid with a DPPC bilayer in the fluid phase at a given range of FA concentrations, using a coarse-grained (CG) model to describe the composite bilayer that allows longer simulation times than usual at the expense of some loss of atomic detail. Thus, they observe that OA disperses homogeneously into the bilayer at all concentrations without inducing significant structural modifications. This could be indicative that the physiological effects produced by the OA are due to interactions occurring at a purely atomic level or that they are restricted to more condensed membrane structures, such as the gel phase. Peters et al.³⁶ have conducted MD simulations to examine the effect of oleic acid and its saturated analogous, stearic acid, on fluid DMPC bilayers at a FA concentration of 20 mol % using an all-atom (AA) model which provides a fully atomistic description of the system. The results of these simulations revealed some changes in the structure and location of the fatty acids within the bilayer depending on their protonation status. Leekumjorn et al.³⁷ have used MD simulations to explore the changes that both saturated (palmitate) and unsaturated (oleate and linoleate) fatty acids produce on fluid 1,2-dioleoyl-*sn*-glycero-3-phosphatidylcholine (DOPC) bilayers upon increasing fatty acid concentrations of up to 25 mol %, using a united-atoms (UA) representation. These simulations show that the unsaturated fatty acids are able to reduce the lipid ordering within the membrane and increase its fluidity, as compared to the saturated fatty acid which promotes a closer packing of the bilayer chains. In a very recent paper, Hoopes et al.⁴⁰ investigate the effect of OA in a ternary ceramide NS/lignoceric acid/cholesterol model for the *Stratum Corneum* at low concentrations of OA, showing small induced changes in the structural properties of this membrane but noticeable variations in the diffusion of some components of the mixture on OA insertion.

Again, very recently, Cerdomí et al.³⁸ have conducted MD simulations to investigate the interactions of a series of oleic acid derivatives substituted at the carbon-2 of the hydrocarbon chain by the methyl and hydroxyl groups, with model 1,2-dielaidoyl-*sn*-glycero-3-phosphoethanolamine (DEPE) membranes. They used a united-atoms model to describe the lipids and carried out the simulations at a unique fatty acid concentration of 5 mol %. The results from this study demonstrate that the OH and CH₃ substituents act as effective modulators of the position of the carboxylate group in the polar region of the lipid bilayer. For the specific case of the 2-hydroxyoleic acid, the hydroxyl group induces a displacement of the fatty acid chains along the bilayer normal

toward the outer side of the membrane. This could be associated with a better packing of the headgroup area, which would account in turn for the observed shift of the L _{α} -to-H_{II} phase transition to higher temperatures and for the subsequent stabilization of the L _{α} phase.¹⁸

To gain a deeper understanding of the changes produced by oleic acid and its derivative 2-hydroxyoleic in lipid membranes, we have conducted MD simulations to study the effects of insertion of these fatty acids in the model phosphatidylcholine (PC) bilayers with different tail lengths, DPPC and DMPC, at increasing concentrations of the fatty acids. These model bilayers are commonly used in theoretical studies of membranes,^{31,32,36,37,41–51} and there is also a certain amount of experimental information available for them.⁵² A united-atoms model is used to describe the lipids and the fatty acids. It provides reliable results at an affordable computational cost, thus allowing us to study a large number of systems with different FA concentrations of up to 45 mol %, compatible with the inclusion of fatty acids in biological membranes^{25,27} and accounting also for the very dense FA regions that can be formed upon phase separation processes within the membranes.⁵³ The effects of the FAs are investigated by determining from the simulations different structural and dynamic properties of the composite bilayers, which include average atomic positions, the area per lipid, the deuterium order parameter and diffusion coefficients of the phospholipids and fatty acid chains, and the permeability of the mixed bilayers to hydrophobic and hydrophilic penetrant species. The paper is divided into sections as follows. In Section II we describe in some detail the theoretical methods used to carry out the MD simulations. The results extracted from the simulations for the different properties of the FA/PC bilayers as a function of the rising FA concentration are presented and discussed in Section III. Finally, in Section IV the conclusions are given.

II. THEORETICAL METHODS

The MD simulations were carried out on bilayers formed by 128 molecules of DMPC (DPPC), 64 in each leaflet, with different concentrations of oleic and 2-hydroxyoleic acids in their protonated forms. The molecular structures of the fatty acids and the phospholipids are shown in Figure 1. We used the protonated form of the acids because their respective pK_a's of about 9–10⁵⁴ are higher than the pH's at which biomembrane experiments are usually carried out, between 5 and 7.³² We also did not include ions in the medium since they have been shown to have a nonsignificant effect on the lipid organization of the bilayers.³⁷ All simulations were performed using the GROMACS 4.0.7⁵⁵ software package, in an NpT ensemble at temperatures of 314 K for DMPC and 325 K for DPPC, which were selected to maintain the bilayer in the fluid liquid-crystalline phase, and at the same pressure of 1 atm for the two lipid bilayers, with periodic boundary conditions in all directions.

The fatty acid concentrations simulated were 0 (pure DMPC and DPPC bilayers), 3, 6, 11, 20, 33, and 45 mol % relative to the bilayer lipids. The initial equilibrated structures of DMPC and DPPC were taken from a recent work by Kukol,⁵⁶ and the fatty acid chains were inserted into these structures using a methodology inspired in the recent works by Notman et al.³² and Peters et al.,³⁶ with some variants to achieve shorter equilibration times while keeping the quality of the simulations. Accordingly, the initial dehydrated membrane was first expanded on the bilayer xy plane to generate enough space to insert the fatty acid chains.

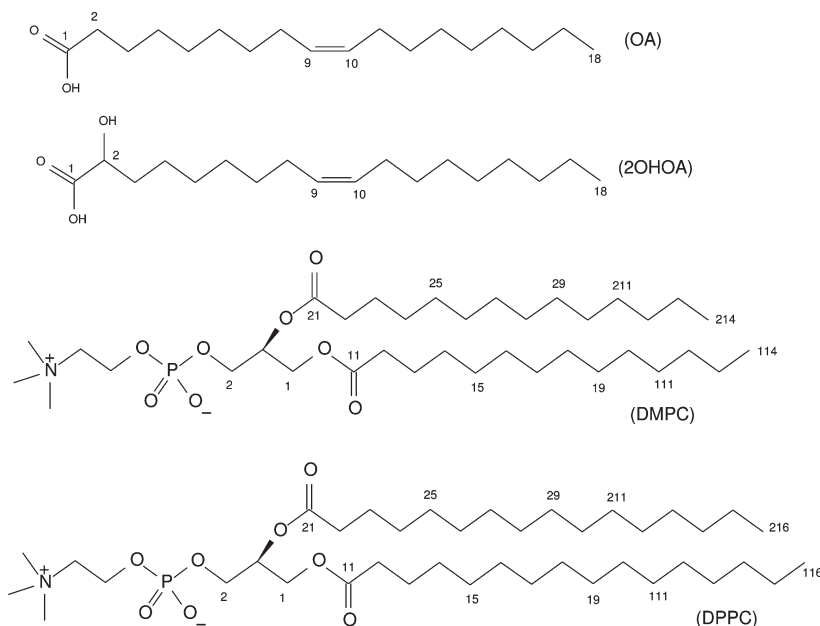


Figure 1. Molecular structures of the OA, 2OHOA, and the DMPC and DPPC phospholipids with partial identification of the atomic positions.

The magnitude of this expansion was estimated from previous information on the area per lipid for similar bilayer systems.³² Next, we calculated for each leaflet the average (x, y) coordinates of every phospholipid and created from them a grid of points on the xy plane that gave the locations of the best gaps for insertions of the acid chains. In each of these gaps, a fatty acid chain was then placed, taken from a conformers library generated previously by simulations of single acid chains with restrained extended conformations in water. The fatty acid chains were inserted along direction z normal to the bilayer, with the same polar orientations as those of the phospholipids and with their average z positions matching the average z positions of the monolayers, plus a random offset between $\pm 2\%$ and $+2\%$ added for greater heterogeneity in the resulting membrane. After setting the vertical positions, the inserted acid chains were rotated around their longitudinal axes to maximize the interatomic distances with the neighboring lipid chains, ruling out those insertions for which the least of these interatomic distances was shorter than 0.8 \AA , a value which ensured stable initial configurations.

After inserting the fatty acids, the system was solvated avoiding the presence of water inside the bilayer. This was done by first generating water molecules randomly in the simulation box using the *genbox* program of the GROMACS package, on the basis of the free space available, and then removing the water molecules generated inside the bilayer between the regions with highest densities of phospholipid polar heads. This produced certain interpenetration in the polar regions, in agreement with the real state of the system,⁵² and prevented the formation of gaps between the water monolayers and the membrane, which may cause problems in the equilibration step. The system was thus solvated with a total of 4000 to 5000 water molecules, depending on the size of the expansion applied, which were distributed in two water layers, one on each side of the lipid membrane, of about 1.5 nm thickness each. The separation between a bilayer and its nearest periodic image was in turn large enough to avoid self-interactions. The resulting structure was then energy minimized using the steepest-descent method and subsequently equilibrated

for 500 ps with a time step of 1 fs. During equilibration, both volume and temperature were held constant using the Berendsen algorithm^{57,58} with a coupling constant τ_T of 0.1 ps, which drove the system toward the desired temperatures of 314 K for DMPC and 325 K for DPPC and eliminated local overpressure. A second equilibration was then performed at both pressure and temperature constants, again using the Berendsen algorithm with $\tau_T = 0.1$ ps and $\tau_p = 1$ ps. This step was maintained for 1 ns, using the LINCS algorithm⁵⁹ to constrain both the phospholipids and fatty acid bonds and the SETTLE⁶⁰ algorithm to constrain the water bonds. These constraints and the stability provided by the pressure and temperature coupling algorithms allowed us to use a time step of 4 fs^{55,61} in all simulations.

The Berendsen algorithm is quite suitable to drive the system toward the desired pressure and temperature, but it samples an ill-defined thermodynamic ensemble,^{61,62} which raises some theoretical issues at determining the thermodynamic properties of the system. For this reason, after equilibration, the Berendsen algorithm was replaced by the Nosé–Hoover thermostat,^{63,64} with $\tau_T = 1$ ps, and by the Parrinello–Rahman barostat,⁶⁵ with $\tau_p = 2$ ps, at the targeted pressure and temperature, respectively, which ensured the sampling of a true NpT ensemble.^{63–65} During the simulations, the structural parameters were constrained in the same way as along the NpT equilibration step. The simulations were run for 100 ns, with the first 10 ns being discarded for analysis to ensure proper equilibration of the system, except for the calculation of the mean square displacement (MSD) curves for which only the first 2 ns was discarded to improve sampling.

During the equilibration and simulation steps, the Lennard-Jones interactions were treated with a cutoff of 1.4 nm, and the electrostatic interactions were calculated using the particle mesh Ewald algorithm⁶⁶ (PME), with a cutoff radius of 0.9 nm for the real part and a grid spacing of 0.14 nm for the reciprocal part, using, moreover, a fourth-order B-spline for interpolation. We should note that the algorithm presented in this work to generate mixed PC/FA bilayer systems is very efficient since it hardly perturbs the initial homogeneous equilibrated bilayer after inserting

the fatty acid chains, thus reducing noticeably the equilibration time and providing the versatility needed for a rapid generation of all the composite bilayer systems studied.

As far as the interaction potentials are concerned, we should note that coarse-grained (CG) models provide too low an atomic resolution for the effects of such similar compounds as oleic and 2-hydroxyoleic acids on the lipidic bilayer to be distinguished. On the other hand, all-atom (AA) models yield fully atomistic details of the system but demand a very high computational effort, as compared with united-atoms (UA) models, without ensuring necessarily much better results.⁶⁷ Accordingly, a UA model was chosen to carry out the simulations in this study. Furthermore, a number of new force fields have been developed in recent years which noticeably improve the description of the lipid bilayers.⁶⁸ We have used in particular the parameters recently derived by Kukol⁵⁶ to represent the phospholipids, which are based on the GROMOS96 force field subset 53a6,⁶⁹ along with the partial charges obtained by Chiu et al.⁷⁰ For the hydrophobic fatty acid chains, we have taken the parameters of the 1-palmitoyl-2-oleoyl-sn-glycero-3-phosphocholine (POPC) phospholipid, also derived by Kukol,⁵⁶ including the torsion potentials by Bachar et al.⁷¹ to describe the double bond. The bond parameters for the polar heads of the fatty acids and for the 2-hydroxyl group were obtained from the PRODRG software,⁷² and the partial charges were calculated from a Mulliken population analysis at the HF/6-31G* level, as done by Chiu et al.⁷⁰ The solvent was explicitly represented using the single-point charge (SPC) model.⁷³

All properties of the PC/FA bilayers analyzed in this work were determined using the different tools included in the GROMACS package. The permeability of the bilayer to polar and nonpolar penetrant molecules, characterized by the excess chemical potential of model hydrophilic and hydrophobic particles of water and methane, respectively, across the bilayer, was calculated using Widom's particle insertion technique.⁷⁴ The penetrant particles were inserted into slices of the simulated cell perpendicular to the bilayer normal to calculate the corresponding potential profile across the bilayer, as proposed by Notman et al.³² For this purpose, we used a slightly modified version of the test particle insertion algorithm implemented in GROMACS, which consists of dividing the system into 15 partitions along the z-axis to perform the insertions in separate runs, and making a number of large enough insertions in every partition to ensure convergence in the chemical potential values. A total of 10^5 insertions per configuration were thus performed, taking configurations every 80 ps along the simulations. To reach convergence in the chemical potential at the edges of the simulation box, where pure solvent is most present, we separately calculated the excess chemical potential from simulations of a system formed by penetrant particles in bulk water at the proper temperature (314 or 325 K). This method properly provided converged excess chemical potentials in the edge regions versus other more computationally demanding techniques such as the use of thicker water layers.

III. RESULTS AND DISCUSSION

The systems analyzed in this study are lipid bilayers in which the fatty acid chains are initially immersed. It is also worthwhile, however, to simulate the process of insertion of the fatty acids placed originally in the aqueous phase into the bilayer. Accordingly, we have run a number of trajectories, four for each fatty acid, that simulate the insertion into the DMPC bilayer of 16 molecules of either OA or 2OHOA, a number which accounts for a FA

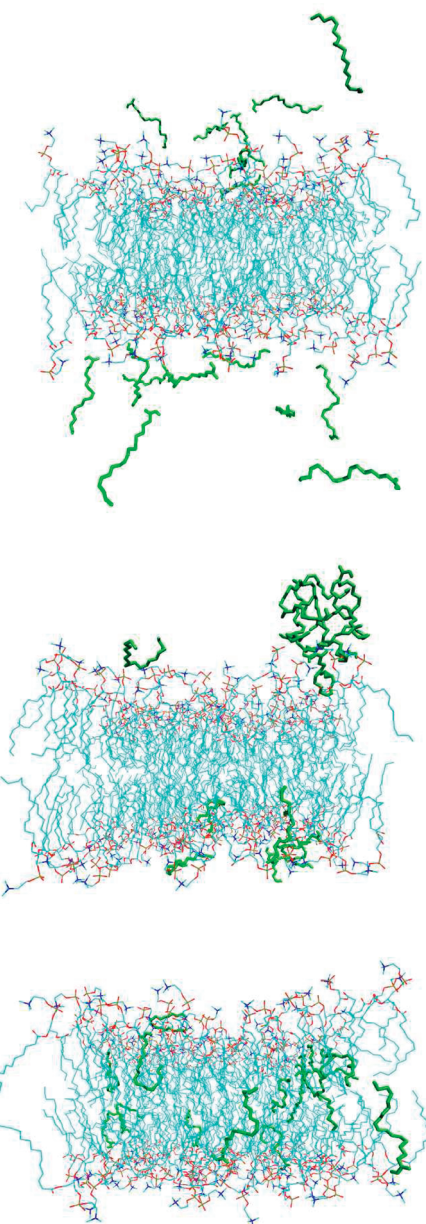


Figure 2. Snapshots of the initial, intermediate, and final configurations corresponding to a trajectory that simulates the insertion of 16 OA molecules (green) into the DMPC lipid membrane (blue). Water molecules are not shown for the sake of clarity.

concentration of 11 mol % relative to lipid content. The insertion of the fatty acid molecules in the DPPC bilayer is supposed to follow the same pattern, due to the similar chemical structure of the two bilayer surfaces.

The insertion simulations were run for 40–60 ns, with different initial random locations of the FA molecules outside the homogeneous bilayer. It was thus observed that insertion of both fatty acids was practically completed in this time scale in the majority of the simulations. FA aggregation in the aqueous phase was also observed to occur in the first steps of all these simulations. These aggregates got close then to the bilayer surfaces and eventually dispersed into the bilayer. In Figure 2, we depict the snapshots of the initial, one intermediate, and the final configurations corresponding to one of the trajectories that simulates

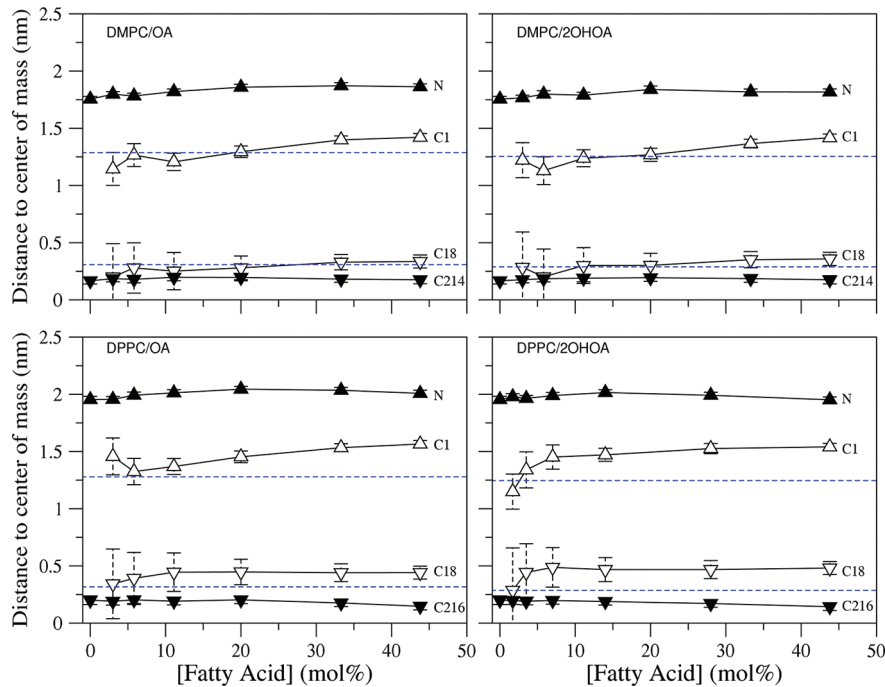


Figure 3. Average atomic positions of selected atoms along the membrane normal relative to the center of mass of the membrane for the four lipid/FA bilayer systems studied, as a function of the FA concentration. For each system, the solid and open symbols represent, respectively, atoms in the bilayers and atoms in the fatty acid molecules. Error bars represent the standard deviations of the average positions over time. Dashed blue lines represent the FA atom positions in the pure FA bilayers.

the insertion of OA molecules in the DMPC membrane, which clearly mimic how the acid chains find their way into the bilayer. Upon insertion, the fatty acids tend to form groups inside the membrane, creating microdomains with high acid concentrations. This behavior could lie behind the explanation of the phase separation that has been observed experimentally in this kind of bilayer system^{25,53,75} and which it has not been able to reproduce by simulations with the fatty acids initially dispersed within the membrane.^{36,32} We should note also that the spontaneous insertion of the FA molecules in the bilayer is in accordance with the experimental evidence that dietary fatty acids eventually end up incorporated into the plasma membranes⁸ and with the observation in model systems that this process is thermodynamically favored.⁷⁶

Let us consider then the simulations of the systems in which the OA and 2OHOA molecules are initially dispersed inside the DMPC and DPPC bilayers. We discuss first the structural properties extracted from the simulations, which include the average atomic positions, the area per lipid, and the order parameter of the hydrophobic chains of phospholipids and the fatty acids within the membrane.

We have calculated the average atomic positions of some selected atoms along the bilayer normal relative to the bilayer center of mass, specifically those of the carboxylic C1 and the tail C18 atoms of the fatty acids, the N atom of both DMPC and DPPC phospholipids, and the tails C214 and C216 atoms of the DMPC and DPPC lipids, respectively (see Figure 1). The average positions were obtained by averaging over all the equivalent atoms in the system and over both leaflets of the bilayer. In Figure 3, we plot the average atomic positions of the selected atoms for the four PC/FA bilayer systems studied, as a function of the FA composition. It is noted here that the average positions of the

fatty acid atoms in the lowest concentration systems (3%) display a large and random variability due to the intrinsic limited amount of atomic positions available to do the statistics; these positions are therefore excluded from the discussion.

Observation of Figure 3 shows then that in all systems the atomic positions of the fatty acids change only slightly on increasing the fatty acid content and that they are lifted toward the polar phospholipid heads, resulting in more extended chain conformations. The addition of a higher number of acid chains does not alter significantly the thickness of the membranes either, calculated as the normal distance from the N atom of the choline group to the center of mass of the bilayer. This indicates that accumulation of OA and 2OHOA inside the membrane does not induce important structural perturbations in the bilayers, in agreement with experimental evidence.²⁵ As for the average positions of the phospholipid atoms, the major difference observed in the two phospholipid bilayers of DMPC and DPPC lies in the lengths of the hydrophobic tails of the phospholipids, which give thicker DPPC bilayers, as shown by the larger distance of the N atom to the center of mass of the bilayer. It is interesting to note also that the atomic positions of the fatty acids are correlated to the atomic positions of the phospholipid polar heads. The average N(PC)–C1(FA) distances in this respect remain practically identical when passing from one PC bilayer to the other for each FA. When comparing, however, these distances for the same PC bilayer containing different fatty acids, it is noticed that 2OHOA is placed slightly closer to the lipid polar head, with the average N(PC)–C1(FA) distance becoming 0.04 Å shorter in systems with the highest, 45%, concentration. In a way, this reveals the importance that the interactions between the fatty acid and the phospholipid polar heads have in fixing the longitudinal location of the fatty acids inside the membrane, as reported previously by Cordomí et al.³⁸ As a consequence, in the

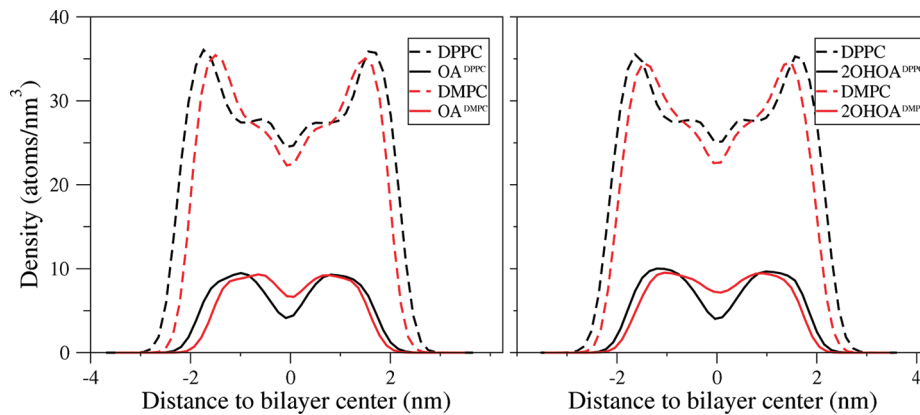


Figure 4. Atomic density distributions of the locations of PC and FA groups along the bilayer normal for a FA concentration of 45 mol %. The left panel corresponds to the PC/OA systems and the right panel to the PC/2OHOA systems. The center of mass is located at $z = 0$.

thicker DPPC membranes, the fatty acid hydrophobic tails are shifted outward from the bilayer center, as noticed by comparing the C1(FA) positions with those in the pure OA and 2OHOA systems given by the dashed blue line in Figure 3. This results in a different composition of the bilayer core region in terms of the FA/PC ratio, an effect that is clearly observed in Figure 4, where the atomic density distributions of the PC and FA groups along the two bilayers for the highest FA concentration of 45 mol % are plotted.

The next structural parameter considered is the average area per lipid of the membranes, which has been calculated as the ratio of the area on the xy plane over the number of lipids on one leaflet including both the phospholipids and the fatty acid chains. In Figure 5 we plot the area per lipid against the fatty acid concentration for the four FA/PC bilayer systems studied. The area per lipid calculated for the homogeneous DMPC and DPPC bilayers is 0.62 nm^2 in both cases, in good agreement with the reported experimental values of around 0.62 and 0.63 nm^2 , respectively.^{77,78} Figure 5 shows that the area per lipid decreases as the FA concentration rises in a practically similar way in the four mixed PC/FA bilayers. This decrease is caused by the smaller transversal section of the fatty acid chains relative to that of the phospholipids and agrees with the behavior of the area per lipid previously reported for similar systems, also by MD simulations.^{32,36} Figure 5 shows also that the decrease of the area per lipid is not linear, which indicates that the fatty acid–bilayer mixture is not ideal. We have extrapolated the ideal behavior of the mixtures from the area per lipid of the homogeneous OA and 2OHOA systems calculated by conducting simulations of the pure bilayers containing 128 FA chains. As observed in Figure 5, the area per lipid of the mixed systems always remains below the ideal values (straight lines in Figure 5). This means that the lipid interactions are comparatively stronger in mixtures than they are in the homogeneous systems, thus highlighting a thermodynamically favored solution, as reported experimentally.⁷⁶

The order parameter accounts for the relative orientation of the methylene groups of the hydrocarbon chains and therefore provides information on the ordering degree of the chains in the bilayer. We have calculated specifically the deuterium order parameter S_{CD} , which accounts for the relative orientation of the C–D bond with respect to the membrane normal⁷⁹ and can be measured by NMR. This parameter is calculated from the simulation using its relationship with the order parameter tensor elements,⁸⁰ which states

$$S_{CD} = \frac{1}{3} (2S_{xx} + S_{yy}) \quad (1)$$

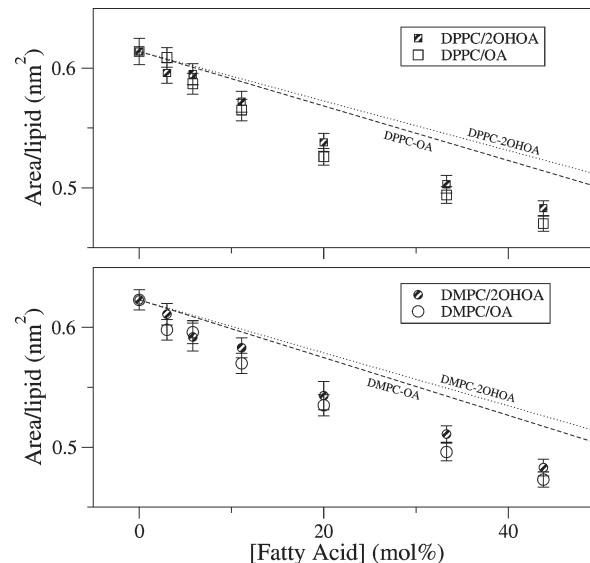


Figure 5. Area per lipid for the four lipid/FA bilayer systems studied as a function of the FA concentration. The expected ideal behaviors are also depicted (gray lines).

where the tensor elements are given by $S_{ii} = 1/2\langle 3 \cos^2 \theta_i - 1 \rangle$ ($i = x, y$), with θ_i being the angle between the bilayer normal and the i th molecular axis, and where $\langle \dots \rangle$ indicates an average over simulation time and over equivalent molecules. The usual conventions are used to define these molecular axes, including those for unsaturated carbons where required.⁸¹ The order parameters take values ranging from 1 to -0.5 as the molecular axis goes from being completely aligned along the bilayer normal to being perpendicular to it and cancels out for random orientation.

In Figure 6, we plot the deuterium order parameters of the phospholipid $sn1$ and $sn2$ hydrocarbon chains extracted from simulations of homogeneous DMPC and DPPC membranes, along with the experimental values reported, respectively, by Petrache et al.⁸² and Douliez et al.⁸³ for each $sn2$ chain of the two phospholipids. As observed, the $|S_{CD}|$ values calculated for the phospholipids agree quite well with the experiment. Upon insertion of the fatty acids into the bilayers, the order parameters of the central atoms of the phospholipids increase, as shown in Figure 7, for the $sn1$ hydrocarbon chain and in Figure S.1 (Supporting Information) for the $sn2$ hydrocarbon chain. This increase is more

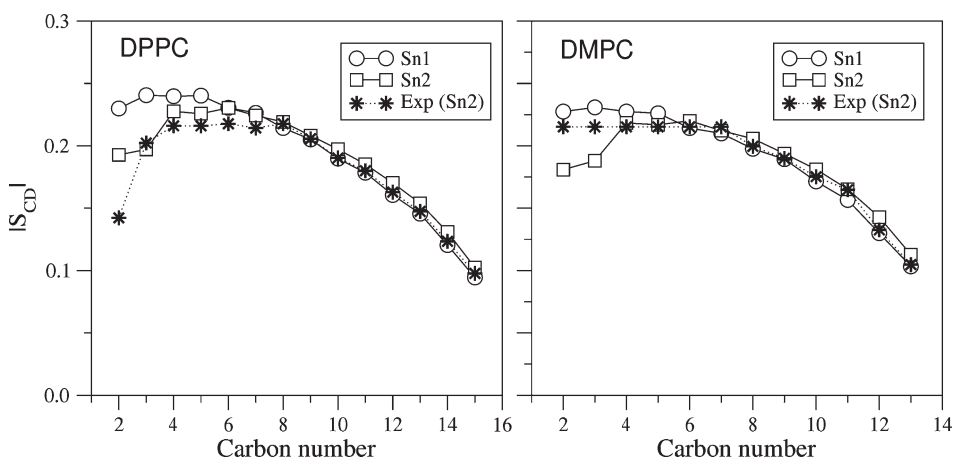


Figure 6. Deuterium order parameters in both *sn1* and *sn2* hydrocarbon chains extracted from simulations of homogeneous DPPC (left panel) and DMPC (right panel) phospholipid bilayers. Experimental values for the *sn2* chains are also included.

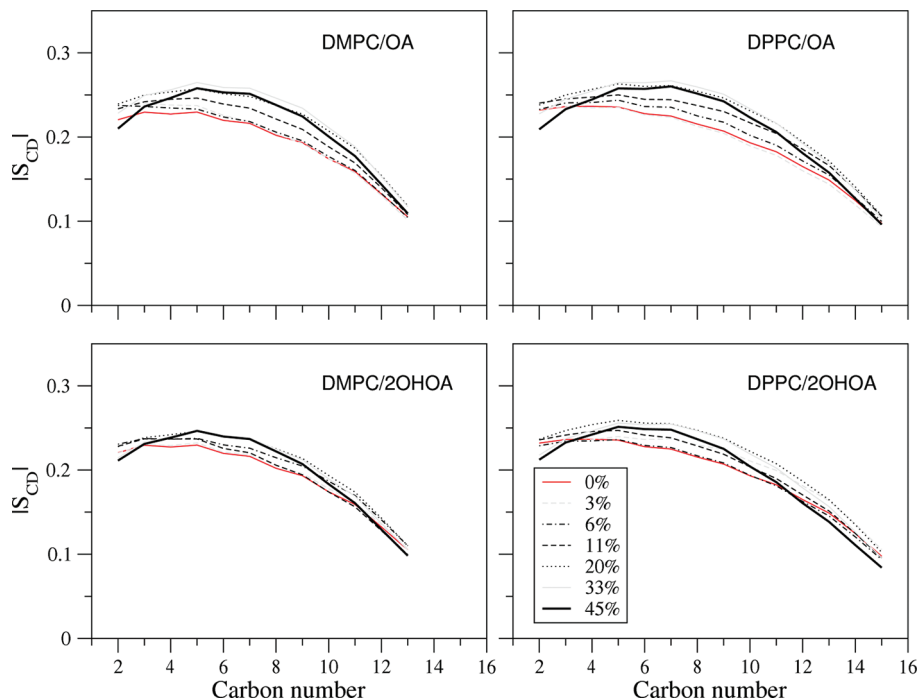


Figure 7. Deuterium order parameters for the *sn1* hydrocarbon chain of each PC lipid in the four lipid/FA bilayer systems studied. The different FA concentrations are identified in the inset, which applies to all systems. Values for the *sn2* chain are shown in the Supporting Information.

pronounced in the case of OA insertion, whereas the type of PC bilayer seems to play no role in this respect. The effect of increasing OA concentration on the phospholipids order is in agreement with that observed by Peters et al.³⁶ also using an atomistic representation of the bilayers and seems to contrast with the increase of the order parameters of the DPPC observed by Notman et al.³² using a CG representation which the authors consider marginal and pending further comparison with experiment.

As far as the order parameters of the fatty acids are concerned, their absolute values do not change much as the acid chains accumulate inside the membranes, as clearly appreciated in Figure 8, where the FA order parameters for the four mixed PC/FA bilayer systems are shown. There is also a reasonable agreement between our calculated values and those reported from experiment for an

oleic chain in POPC around the unsaturation,⁸⁴ which show a minimum at carbon 10 with a value around zero. We observe in Figure 8 that the deuterium order parameters of the fatty acid carbons hardly change with the fatty acid concentration, except for the case of the double-bonded C9 carbon, in which the order parameter slightly increases as the FA concentration rises. The FA order parameter profiles for the two DMPC and DPPC bilayers with a high content of OA are quite similar, as are the profiles for the two lipid bilayers containing high concentrations of 2OHOA. This indicates that the polar head conformations of the fatty acid inside either the DMPC or the DPPC bilayers are practically the same, in agreement with our previous discussion on the atomic positions. When comparing the same bilayers containing different FAs, it is observed first in Figure 8 that the

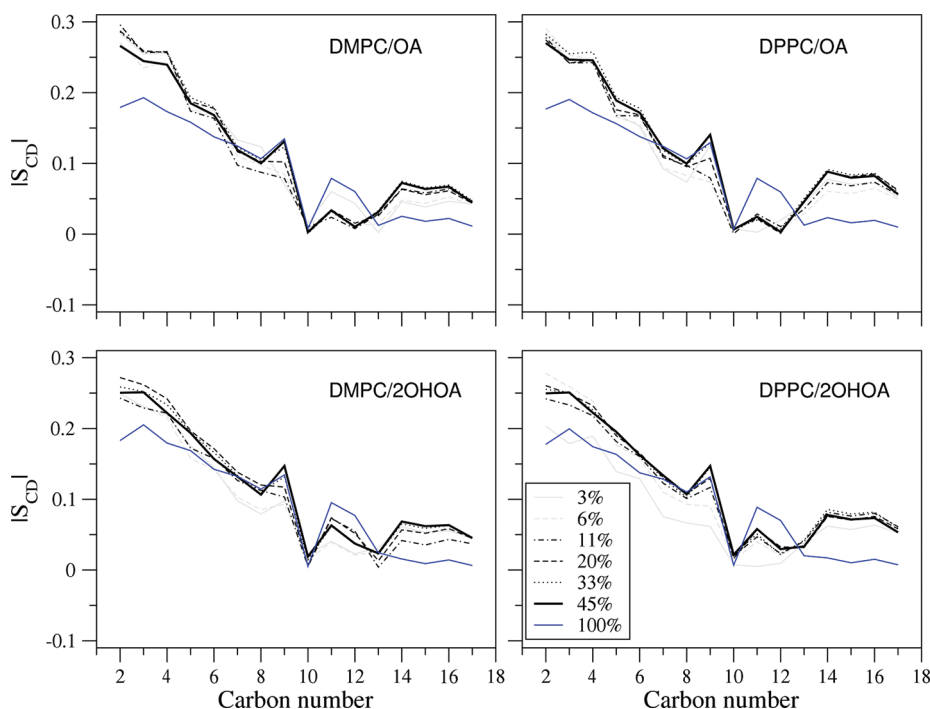


Figure 8. Deuterium order parameters for the FA hydrocarbon chains in the four lipid/FA bilayer systems studied. The different FA concentrations are identified in the inset, which applies to all the systems.

S_{CD} values of the carbon atoms located in the polar region are different for OA and 2OHOA systems, a result that could be interpreted as different interactions of both OA and 2OHOA with the phospholipid polar head. Second, in the vicinity of the double bond, joining the C9 and C10 atoms, the S_{CD} value for the C9 atom is comparatively higher in the 2OHOA-based systems, and in contrast, the $|S_{CD}|$ values for the C11 to C13 carbons are higher in the OA systems. This could also be due to different interactions of the FAs with the bilayer. It is noteworthy that these FA order parameter profiles are indeed very similar in pure OA and 2OHOA bilayer, and OA suffers larger deviations in the carbons around the double bond when mixed in the lipid bilayer.

Let us consider now the dynamic properties of the mixed membranes. We have calculated first the lateral diffusion coefficient of the phospholipids and fatty acids from the gradients of the mean square displacements (MSDs) as a function of time. The MSD values for the phospholipids were obtained by averaging over the displacements of all the phospholipid atoms, which is equivalent to averaging over the displacements of the center of mass of each phospholipid since the slope of the linear region of the MSD curve is the same in both cases.⁸⁵ To account for the relative motions of the lipid and water monolayers with respect to each other, which give rise to artifacts in the simulations due to the finite size of the box and to the periodic boundary conditions,⁸⁵ we have removed the center of mass motion of each bilayer from the trajectory before calculating the MSD curves.^{61,85–87} Concretely, we have first separately calculated the MSD curves over time for each monolayer, then subtracted their corresponding center of mass motions, and eventually averaged the two MSD curves to obtain diffusion coefficients. The error of the diffusion coefficients was estimated as half the difference of the diffusion coefficients obtained for each monolayer.

The values of the diffusion coefficients for both DMPC and DPPC phospholipids as a function of the FA concentration are

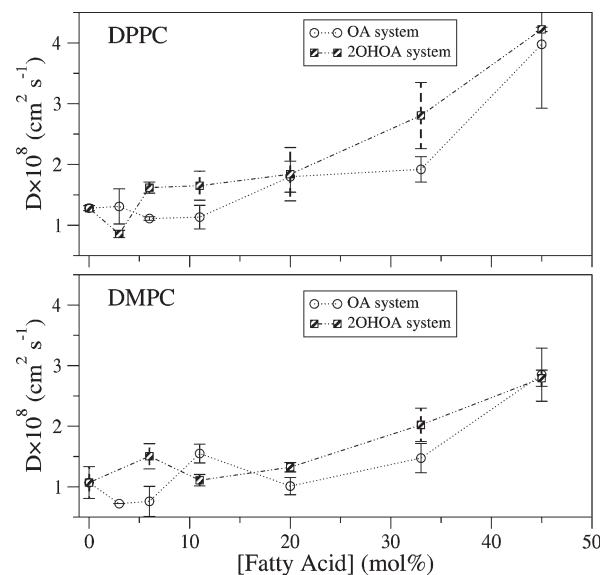


Figure 9. Lateral diffusion coefficients of the DPPC (upper panel) and the DMPC (lower panel) bilayers calculated from the MSD curves of the phospholipid atoms as a function of the fatty acid concentration.

plotted in Figure 9. As observed, the values obtained for the thicker DPPC bilayer display a large variability. This variability arises from the different diffusion constants obtained in each separated monolayer since the corresponding MSD plots, which are included in the Supporting Information (Figures S2–S6), are well converged. In contrast, the diffusion coefficients for the DMPC bilayers are reasonably well correlated in the two monolayers. In both cases, the diffusion coefficients clearly increase for concentrations of the FAs higher than 20 mol %, an increase which is greater in the DPPC systems. This increase is presumably

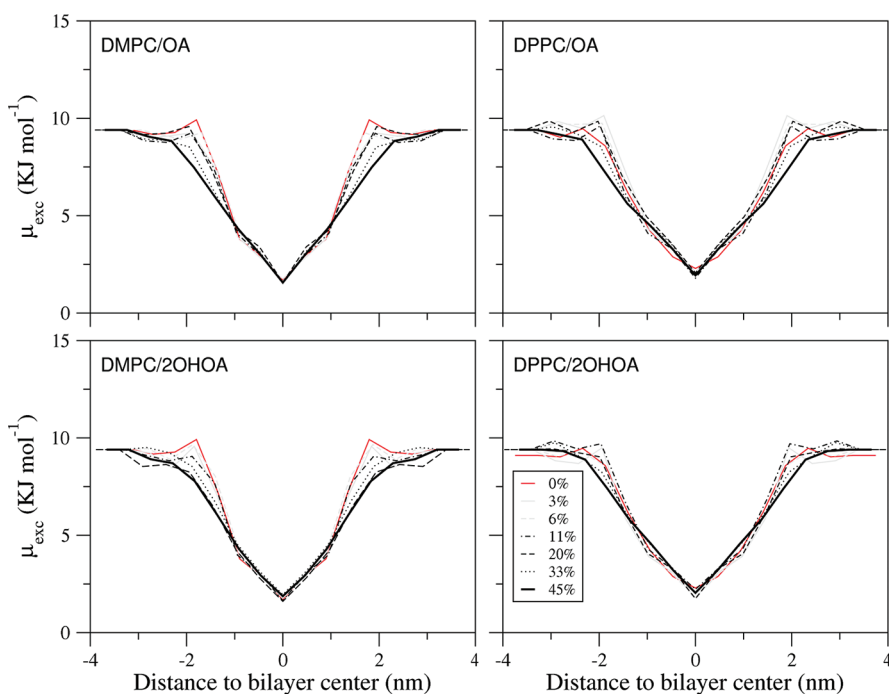


Figure 10. Excess chemical potential profiles of a hydrophobic methane particle along the bilayer normal for the four lipid/FA bilayer systems studied. The different FA concentrations are identified in the inset, which applies to the four systems.

due to a fluidization effect of the inserted FA chains at large concentrations supported by the remarkably high values of the diffusion coefficients calculated for the homogeneous OA ($[63 \pm 6] \times 10^{-8} \text{ cm}^2 \text{ s}^{-1}$) and 2OHOA ($[66 \pm 9] \times 10^{-8} \text{ cm}^2 \text{ s}^{-1}$) systems. There are not, however, significant differences in the mobility of the lipids as a consequence of the insertion of either the oleic or the 2-hydroxyoleic fatty acids, also in agreement with the very similar diffusion coefficients found in the homogeneous systems. Furthermore, these results are in agreement with those reported by Notman et al.³² from molecular dynamics simulations of DPPC/OA systems using a coarse grain model that allows much longer simulation times.

We should note also that the substantial changes observed in the diffusion of the phospholipids at high FA concentrations correlate well with the structural modifications accounted for by the reported deuterium order parameters (Figure 7), which significantly deviate from their values in the homogeneous bilayers. This indicates that significant structural changes take place in systems with high FA concentrations (>20 mol %). It is also observed that while both the area per lipid and the order parameters suggest a packing effect due to the thermodynamically favored mixture the diffusion coefficient, driven by the FA-induced fluidization, shows a higher mobility of the chains inside the bilayer. This 2-fold impact on the membrane could play an important role in the phase behavior of these kinds of mixed systems.

As far as the lateral diffusion coefficients of the FA molecules in the bilayers is concerned, although the statistics in this case are poorer in the case of low concentrations due to the smaller number of FA chains, it is observed that the diffusion of the FAs is faster than that of the phospholipids and that it increases as the fatty acid concentration rises. For the bilayer systems with the highest FA concentration of 45 mol %, which give the best converged MSD curves, the diffusion coefficients of the FA molecules obtained for each system are $[4.7 \pm 0.2] \times 10^{-8} \text{ cm}^2 \text{ s}^{-1}$ (DMPC/OA), $[4.6 \pm 0.6] \times 10^{-8} \text{ cm}^2 \text{ s}^{-1}$

(DMPC/2OHOA), $[6.8 \pm 0.9] \times 10^{-8} \text{ cm}^2 \text{ s}^{-1}$ (DPPC/OA), and $[6.7 \pm 0.1] \times 10^{-8} \text{ cm}^2 \text{ s}^{-1}$ (DPPC/2OHOA). According to these values, the mobility of both FAs is similar in each bilayer and increases for both when passing from the DMPC to the DPPC bilayer.

The second dynamic property analyzed is the permeability of the PC/FA bilayers to both a penetrant hydrophobic particle of methane and a penetrant hydrophilic particle of water. This property is related to the excess chemical potential of the particle along the bilayer normal, which was calculated using the Widom particle insertion, as indicated in Section II. The chemical potential profiles obtained for the particle of methane along the bilayer normal in the four PC/FA bilayers studied at the different FA compositions are shown in Figure 10. As expected, in the case of a hydrophobic particle all the profiles show a minimum in the hydrophobic core of the bilayer, where the interactions between the methane particle and the hydrophobic tails are stronger, with maxima in the edge regions of the bilayers. Some changes in these profiles are then observed in the polar regions of the bilayers for systems with higher FA concentrations, which consist basically of a decrease in the chemical potentials in these regions. It is noteworthy that the most important variations in the energetic profiles occur around the location of the FA polar heads. It thus becomes clear that the interactions of the FA polar heads with the bilayer play an important role in the alteration of the chemical potential profiles of the penetrant hydrophobic molecules. Furthermore, the effect produced by the two fatty acids, OA and 2OHOA, in this sense seems to be similar in both DMPC and DPPC bilayers.

As for the penetrant hydrophilic particle of water, the chemical potential profiles shown in Figure 11 display the completely opposite behavior, with the barrier located in the center of the bilayer. The influence of the FA chains in this region is more residual, as evidenced by the fact that the barrier height remains constant in all systems. Nevertheless, some broadening of the

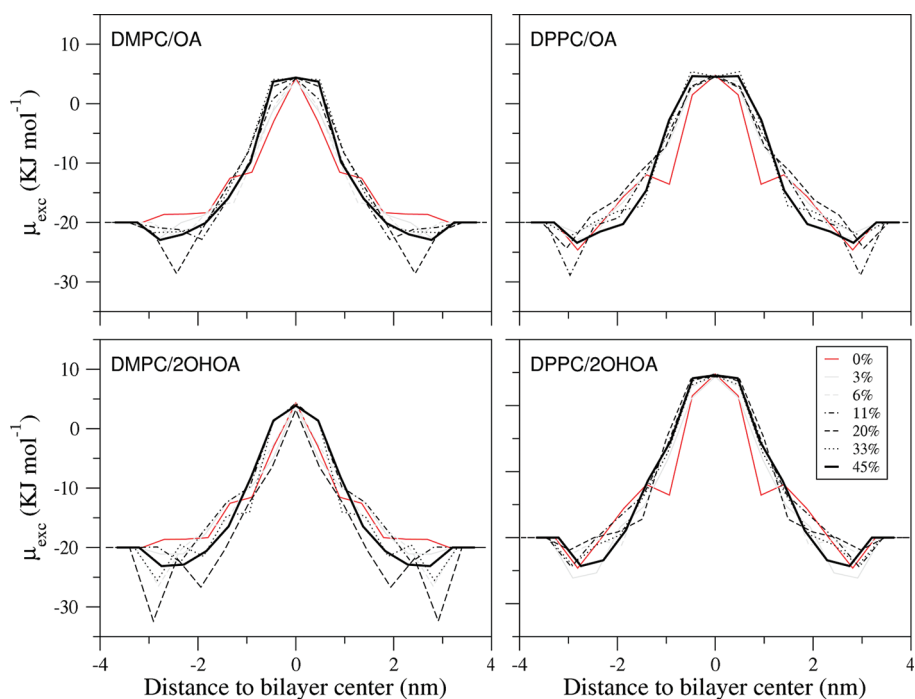


Figure 11. Excess chemical potential profiles of a hydrophilic water particle along the bilayer normal for the four lipid/FA bilayer systems studied. The different FA concentrations are identified in the inset, which applies to the four systems.

barrier is observed as the concentration of FA increases, which might be somehow related to the change in lipid composition inside the bilayer noticed above in the analysis of the structural properties. In any case, the results of our simulations indicate that the chemical potential profiles of water are not significantly altered by the presence of the fatty acids in the bilayers, in agreement with the results reported by Notman et al.³²

IV. CONCLUSIONS

In this work, we have studied by MD simulations the possible structural and dynamical modifications induced by the presence of the oleic and 2-hydroxyoleic fatty acids at rising concentrations in model DMPC and DPPC phospholipid bilayers. We have simulated first the process of insertion of the fatty acids in the bilayers from the aqueous phase and observed that this process is feasible and that it can be hindered upon the stability of the FA aggregates formed in the aqueous phase. It is also observed that the insertion process of the FA results in the creation of micro-domains with high FA concentrations indicating a certain degree of phase separation within the membrane, which is in agreement with experimental evidence. A deeper insight into these insertion processes would be provided by calculating the relative stability of FA aggregates formed and also by comparison of the potential mean force (PMF) along the FA insertion pathways for OA and 2OHOA, and work in this sense is now under way.

We have then analyzed the variation of a number of structural and dynamic properties of the membranes as a function of the fatty acid concentration. These properties include the location of the chains inside the membrane, the area per lipid, the deuterium order parameter, the lateral diffusion coefficient of the fatty acid and phospholipid molecules, and the permeability of the bilayers to nonpolar penetrants. As for the atomic positions of the fatty acid chains inside the bilayers, it has been shown that the polar heads of both OA and 2OHOA acids locate slightly below the phospholipid

polar heads and at closer distances as the FA concentration increases, irrespective of the membrane thickness. This is indicative of the importance of the interactions between the polar heads in fixing the position of the fatty acid chains across the bilayers. This structural conclusion is further validated by the values of the deuterium order parameter extracted from the simulations, which clearly show that the structure of OA inside the bilayer differs from that of 2OHOA but is very similar in both DPPC and DMPC bilayers. As the fatty acid concentration rises, the area per lipid of the membrane decreases as a consequence of the smaller transversal area of the chains inserted into the PC bilayers. This decrease in addition deviates from the linearity, indicating that the fatty acid–bilayer mixtures are not ideal and are thermodynamically favored.

Our simulations also show that high levels of fatty acid can induce slight modifications in the dynamical properties of the membranes. In particular, the lateral diffusion of both the phospholipid and fatty acid chains increases as the fatty acid concentration rises, which relates to an enhancement of the fluidity of the membranes. This increase is found to be more significant in the thicker DPPC systems, while the effect of OA and 2OHOA seems to be similar. Also, the excess chemical potential of the hydrophobic particle of methane across the bilayer, which is used to characterize permeability of the membranes to both hydrophobic (methane) and hydrophilic (water) penetrants, undergoes some alterations as the fatty acid concentration increases.

In general, the changes induced in the bilayers by the oleic and 2-hydroxyoleic acids do not differ much. The bilayer alterations described in this work are clearly far from justifying on their own the important therapeutic properties of the oleic acid nor those recently reported of the 2-hydroxyoleic acid. Nevertheless, these alterations provide some interesting information on these systems at the atomic level that allows us to devise to additional lines of research. In this sense, the atomistic level used in this work to describe the systems formed by PC phospholipids and OA and

2OHOA fatty acids might be used to investigate in detail, by molecular dynamics simulations, the possible phase transitions that may take place upon insertion of fatty acids in the membrane, which have been shown to play an important role in the interactions between the bilayer and membrane proteins.¹⁹ It would also be worthwhile to study systems which include membrane proteins, given the predominant role played by these structures in the membrane lipid therapies.³ The use of the force field developed by Kukol,⁵⁶ in which both proteins and lipid bilayers are properly described, opens immediately the door to these kind of membrane protein studies in which our group is currently involved.

■ ASSOCIATED CONTENT

5 Supporting Information. A figure showing the order parameters of the *sn*2 PC chains which complements Figure 7 for the *sn*1 chains along with the MDS plots from which the diffusion constants are calculated and the topology files for oleic and 2-hydroxyoleic acids used with GROMACS 4.0.7. This material is available free of charge via the Internet at <http://pubs.acs.org>.

■ AUTHOR INFORMATION

Corresponding Author

*E-mail: jcbl@um.es (J. C.); zuniga@um.es (J. Z.); rqna@um.es (A. R.).

■ ACKNOWLEDGMENT

This work was partially supported by the Spanish Ministerio de Ciencia e Innovación under Projects CTQ2011-25872 and CONSOLIDER CSD2009-00038 and by the Fundación Séneca del Centro de Coordinación de la Investigación de la Región de Murcia under Project 08735/PI/08. J.C. acknowledges a FPU fellowship provided by the Ministerio de Educación y Ciencia of Spain, and J.P.C.C acknowledges the fellowship provided by the Fundación Séneca Agencia de Ciencia y Tecnología de la Región de Murcia, within its Postdoctoral Research Staff Training Program. Fundación Parque Científico de Murcia is also acknowledged for the allocated computational time on their supercomputing facilities and for technical support.

■ REFERENCES

- (1) Kusumi, A.; Pasenkiewicz-Gierula, M. *Biochemistry* **1988**, *27*, 4407.
- (2) Escribá, P. V.; González-Rosb, J. M.; Goni, F. M.; Vigh, L.; Sánchez-Magraner, L.; Kinnunen, P. K. J.; Fernández, A. M.; Busquets, X.; Horváth, I.; Barceló-Coblijn, G. *J. Cell. Mol. Med.* **2008**, *12*, 829.
- (3) Escribá, P. V. *Trends Mol. Med.* **2006**, *12*, 34.
- (4) Pagnan, A.; Coroche, R.; Ambrosio, G. B.; Ferrari, S.; Guarini, P.; Piccolo, D.; Opportuno, A.; Bassi, A.; Olivieri, O.; Baggio, G. *Clin. Sci.* **1989**, *76*, 87.
- (5) Vicario, I. M.; Malkova, D.; Lund, E. K.; Johnson, I. T. *Ann. Nutr. Metab.* **1998**, *42*, 160.
- (6) Zicha, J.; Kunes, J.; Devynck, M. A. *Am. J. Hypertens.* **1999**, *12*, 315.
- (7) Escribá, P. V.; Sanchez-Dominguez, J. M.; Alemany, R.; Perona, J. S.; Ruiz-Gutiérrez, V. *Hypertension* **2003**, *41*, 176.
- (8) Escudero, A.; Montilla, J. C.; García, J. M.; Sanchez-Quevedo, M. C.; Periago, J. L.; Hortelano, P.; Suarez, M. D. *Biochim. Biophys. Acta* **1998**, *1394*, 65.
- (9) Dominiczak, A. F.; McLaren, Y.; Kusel, J. R.; Ball, D. L.; Goodfriend, T. L.; Bohr, D. F.; Reid, J. L. *Am. J. Hypertens.* **1993**, *6*, 1003.
- (10) Martin-Moreno, J. M.; Willett, W. C.; Gorgojo, L.; Banegas, J. R.; Rodríguez-Artalejo, F.; Fernández-Rodríguez, J. C.; Maisonneuve, P.; Boyle, P. *Int. J. Cancer* **1994**, *58*, 774.
- (11) Tzonou, A.; Lipworth, L.; Kalandidi, A.; Trichopoulou, A.; Gamatsi, L.; Hsieh, C.-C.; Notara, V.; Trichopoulos, D. *Br. J. Cancer* **1996**, *73*, 1284.
- (12) Ruiz-Gutiérrez, V.; Muriana, F. J. G.; Guerrero, A.; Cert, A. M.; Villar, J. *J. Hypertens.* **1996**, *14*, 1483.
- (13) Hardman, W. E. *J. Nutr.* **2004**, *134*, 3427S.
- (14) Alemany, R.; Terés, S.; Baamonde, C.; Benet, M.; Vogler, O.; Escribá, P. V. *Hypertension* **2004**, *43*, 249.
- (15) Alemany, R.; Vogler, O.; Terés, S.; Egea, C.; Baamonde, C.; Barcelo, F.; Delgado, C.; Jakobs, K. H.; Escribá, P. V. *J. Lipid Res.* **2006**, *47*, 1762.
- (16) Martínez, J.; Gutierrez, A.; Casas, J.; Llado, V.; Lopez-Bellan, A.; Besalduch, J.; Dopazo, A.; Escribá, P. *J. Pharmacol. Exp. Ther.* **2005**, *315*, 466.
- (17) Borchert, G. H.; Giggey, M.; Kolar, F.; Wong, T. M.; Backx, P. H.; Escribá, P. V. *Am. J. Physiol. Heart Circ. Physiol.* **2008**, *294*, HI948.
- (18) Barceló, F.; Prades, J.; Funari, S. S.; Frau, J.; Alemany, R.; Escribá, P. V. *Mol. Membr. Biol.* **2004**, *21*, 261.
- (19) Vogler, O.; Casas, J.; Capo, D.; Nagy, T.; Borchert, G.; Martorell, G.; Escribá, P. V. *J. Biol. Chem.* **2004**, *279*, 36540.
- (20) Prades, J.; Alemany, R.; Perona, J. S.; funari, S. S.; Vogler, O.; Ruiz-Gutiérrez, V.; Escribá, P. V.; Barcelo, F. *Mol. Membr. Biol.* **2008**, *25*, 46.
- (21) Negelmann, L.; Pish, S.; Bornscheuer, U.; Schmid, R. D. *Chem. Phys. Lipids* **1997**, *90*, 117.
- (22) Wartewig, S.; Neubert, R.; Retting, W.; Hesse, K. *Chem. Phys. Lipids* **1998**, *91*, 145.
- (23) Langner, M.; Hui, S. *Biochim. Biophys. Acta* **2000**, *1463*, 439.
- (24) Öörni, M. T. H. K.; Kovanen, P. T.; Ala-Korpela, M. *Biophys. J.* **2001**, *80*, 565.
- (25) Inoue, T.; Yanagihara, S.; Misono, Y.; Suzuki, M. *Chem. Phys. Lipids* **2001**, *109*, 117.
- (26) Castelli, F.; Caruso, S.; Uccella, N. *J. Agric. Food Chem.* **2003**, *51*, 851.
- (27) Funari, S. S.; Barceló, F.; Escribá, P. V. *J. Lipid Res.* **2003**, *44*, 567.
- (28) Prades, J.; Funari, S. S.; Escribá, P. V.; Barceló, F. *J. Lipid Res.* **2003**, *44*, 1720.
- (29) Hac-Wydro, K.; Wydro, P. *Chem. Phys. Lipids* **2007**, *150*, 66.
- (30) Hac-Wydro, K.; Jedrzejek, K.; Dynarowicz-Latka, P. *Colloids Surf, B* **2009**, *72*, 101.
- (31) Knecht, V.; Mark, A. E.; Marrink, S. J. *J. Am. Chem. Soc.* **2006**, *128*, 2030.
- (32) Notman, R.; Noro, M. G.; Anwar, J. *J. Phys. Chem. B* **2007**, *111*, 12748.
- (33) Wong-ekkabut, J.; Xu, Z.; Triampo, W.; Tang, I.; Tieleman, D.; Monticelli, L. *Biophys. J.* **2007**, *93*, 4225.
- (34) Jenske, R.; Lindstrom, F.; Grobner, G.; Vetter, W. *Chem. Phys. Lipids* **2008**, *154*, 26.
- (35) Makyla, K.; Paluch, M. *Colloids Surf, B* **2009**, *71*, 50.
- (36) Peters, G. H.; Hansen, F. Y.; Møller, M. S.; Westh, P. *J. Phys. Chem. B* **2009**, *113*, 92.
- (37) Leekumjorn, S.; Cho, H. J.; Wu, Y.; Wright, N. T.; Sum, A. K.; Chan, C. *Biochim. Biophys. Acta* **2009**, *1788*, 1508.
- (38) Cordomi, A.; Prades, J.; Frau, J.; Vogler, O.; Funari, S. S.; Perez, J. J.; Escribá, P. V.; Barceló, F. *J. Lipid Res.* **2010**, *51*, 1113.
- (39) Nelson, D.; Cox, M. *Lehninger Principles of Biochemistry*; Freeman: New York, 2005.
- (40) Hoopes, M. I.; Noro, M. G.; Longo, M. L.; Faller, R. *J. Phys. Chem. B* **2011**, *115*, 3164.
- (41) Berger, O.; Edholm, O.; Jahnig, F. *Biophys. J.* **1997**, *72*, 2002.
- (42) Hofsaß, C.; Lindahl, E.; Edholm, O. *Biophys. J.* **2003**, *84*, 2192.
- (43) Notman, R.; Noro, M. G.; O'Malley, B.; Anwar, J. *J. Am. Chem. Soc.* **2006**, *128*, 13982.
- (44) Gurtovenko, A. A.; Anwar, J. *J. Phys. Chem. B* **2007**, *111*, 10453.
- (45) López-Cascales, J. J.; Otero, T. F.; Smith, B. D.; Gonzales, C.; Márquez, M. *J. Phys. Chem. B* **2006**, *110*, 2358.
- (46) Leekumjorn, S.; Sum, A. K. *Biochim. Biophys. Acta* **2007**, *1768*, 354.
- (47) Cordomi, A.; Edholm, O.; Perez, J. J. *J. Comput. Chem.* **2007**, *28*, 1017.
- (48) Cordomi, A.; Perez, J. J. *J. Phys. Chem. B* **2007**, *111*, 7052.

- (49) Cordomi, A.; Edholm, O.; Perez, J. *J. Phys. Chem. B* **2008**, *112*, 1397.
- (50) Kepczynski, M.; Kumorek, M.; Stepniewski, M.; Rog, T.; Kozik, B.; Jamrz, D.; Bednar, J.; Nowakowska, M. *J. Phys. Chem. B* **2010**, *114*, 15483.
- (51) Witzke, S.; Duelund, L.; Kongsted, J.; Petersen, M.; Mouritsen, O. G.; Khandelia, H. *J. Phys. Chem. B* **2010**, *114*, 15825.
- (52) Tielemans, D. P.; Marrink, S. J.; Berendsen, H. J. C. *Biochim. Biophys. Acta* **1997**, *1331*, 235.
- (53) Ongpipattanakul, B.; Burnette, R.; Potts, R.; Francoeur, M. *Pharm. Res.* **1991**, *8*, 350.
- (54) Kanicky, J. R.; Shah, D. O. *J. Colloid Interface Sci.* **2002**, *256*, 201.
- (55) Hess, B.; Kutzner, C.; van der Spoel, D.; Lindahl, E. *J. Chem. Theory Comput.* **2008**, *4*, 435.
- (56) Kukol, A. *J. Chem. Theory Comput.* **2009**, *5*, 615.
- (57) Berendsen, H. J. C.; Postma, J. P. M.; DiNola, A.; Haak, J. R. *J. Chem. Phys.* **1984**, *81*, 3684.
- (58) Berendsen, H. J. C. *Computer Simulations in Material Science*; Kluwer: Boston, MA, 1991; Chapter Transport properties computed by linear response through weak coupling to a bath, pp 139–155.
- (59) Hess, B.; Bekker, H.; Berendsen, H. J. C.; Fraaije, J. G. E. M. *J. Comput. Chem.* **1997**, *18*, 1463.
- (60) Miyamoto, S.; Kollman, P. A. *J. Comput. Chem.* **1992**, *13*, 952.
- (61) Anezo, C.; de Vries, A. H.; Holtje, H. D.; Tielemans, D. P.; Marrink, S. J. *J. Phys. Chem. B* **2003**, *107*, 9424.
- (62) Lingenheil, M.; Denschlag, R.; Reichold, R.; Tavan, P. *J. Chem. Theory Comput.* **2008**, *4*, 1293.
- (63) Nosé, S. *Mol. Phys.* **1984**, *52*, 255.
- (64) Hoover, W. G. *Phys. Rev. A* **1985**, *31*, 1695.
- (65) Parrinello, M.; Rahman, A. *J. Appl. Phys.* **1981**, *52*, 7182.
- (66) Darden, T.; York, D.; Pedersen, L. *J. Chem. Phys.* **1993**, *98*, 10089.
- (67) Tielemans, D. P.; MacCallum, J. L.; Ash, W. L.; Kandt, C.; Xu, Z.; Monticelli, L. *J. Phys.: Condens. Matter* **2006**, *18*, S1221.
- (68) Lyubartsev, A. P.; Rabinovich, A. L. *Soft Matter* **2011**, *7*, 25.
- (69) Oostenbrink, C.; Villa, A.; Mark, A. E.; van Gunsteren, W. F. *J. Comput. Chem.* **2004**, *25*, 1656.
- (70) Chiu, S. W.; Clark, M.; Balaji, V.; Subramaniam, S.; Scott, H. L.; Jakobsson, E. *Biophys. J.* **1995**, *69*, 1230.
- (71) Bachar, M.; Brunelle, P.; Tielemans, D. P.; Rauk, A. *J. Phys. Chem. B* **2004**, *108*, 7170.
- (72) Schuttekkopf, A. W.; van Aalten, D. M. F. *Acta Crystallogr.* **2004**, *D60*, 1355.
- (73) Berendsen, H. J. C.; Postma, J. P. M.; van Gunsteren, W. F.; Hermans, J. In *Intermolecular Forces*; Reidel: Dordrecht, The Netherlands, 1981; Chapter Interaction models for water in relation to protein hydration, p 331.
- (74) Widom, B. *J. Chem. Phys.* **1963**, *39*, 2802.
- (75) Busquets, M. A.; Mestres, C.; Alsina, M. A.; Antón, J. M.; Reig, F. *Thermochim. Acta* **1994**, *232*, 261.
- (76) Hoyrup, P.; Davidsen, J.; Jorgensen, K. *J. Phys. Chem. B* **2001**, *105*, 2649.
- (77) Nagle, J. F.; Tristram-Nagle, S. *Biochim. Biophys. Acta* **2000**, *1469*, 159.
- (78) Kucerka, N.; Liu, Y.; Chu, N.; Petracche, H. I.; Tristram-Nagle, S.; Nagle, J. F. *Biophys. J.* **2005**, *88*, 2626.
- (79) Tielemans, D. P.; Berendsen, H. J. C. *J. Chem. Phys.* **1996**, *105*, 4871.
- (80) Egberts, E.; Berendsen, H. J. C. *J. Chem. Phys.* **1988**, *89*, 3718.
- (81) Heller, H.; Schaefer, M.; Schulten, K. *J. Phys. Chem.* **1993**, *97*, 8343.
- (82) Petracche, H. I.; Dodd, S. W.; Brown, M. F. *Biophys. J.* **2000**, *79*, 3172.
- (83) Douliez, J. P.; Leonard, A.; Dufourc, E. *J. Biophys. J.* **1995**, *68*, 1727.
- (84) Seelig, J.; Waespe-Sarcevic, N. *Biochemistry* **1978**, *17*, 3310.
- (85) Wohlert, J.; Edholm, O. *J. Chem. Phys.* **2006**, *125*, 204703.
- (86) Patra, M.; Karttunen, M.; Hyvonen, M. T.; Falck, E.; Vattulainen, I. *J. Phys. Chem. B* **2004**, *108*, 4485.
- (87) Lindahl, E.; Edholm, O. *J. Chem. Phys.* **2001**, *115*, 4938.